

## SPATIAL DISTRIBUTION OF OUTDOOR HEAT STRESS UNDER HEATWAVE CONDITIONS IN SUB-TROPICAL HIGH-DENSITY URBAN ENVIRONMENT

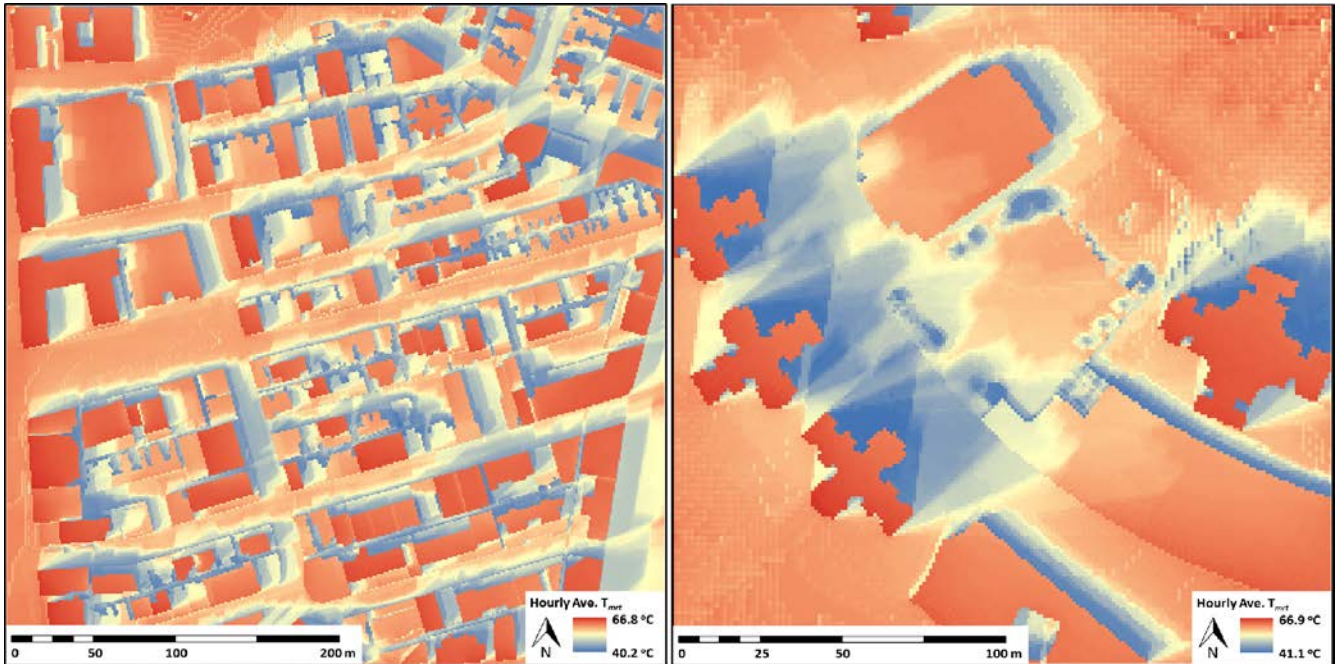


Fig 1: Spatial variation of  $T_{mrt}$  under heatwave conditions (daily maximum air temperature above 33°C).

### Research summary

The magnitude and frequency of heatwaves are expected to increase in the future due to the effect of climate change. Such an enormous thermal load will be further intensified due to the effect of urban structures and results in thermal discomfort or heat stress to pedestrians. One of the design solutions is to provide shading to pedestrians through increasing building height and density as well as vegetation such as street trees. In sub-tropical high-density cities like Hong Kong, tree planting is generally limited due to the limited availability of land. It is therefore important to identify areas which experience the most intense thermal load (i.e. hotspot areas) for the implementation of mitigation measures. In the present study, the spatial distribution of outdoor heat stress, using mean radiant temperature ( $T_{mrt}$ ) as an indicator, is identified using the SOLar and LongWave Environmental Irradiance Geometry (SOLWEIG) model under heatwave conditions. Field measurements of three-dimensional radiation fluxes are used to evaluate model performance. It is found that the model is generally successful to capture the diurnal variation of both shortwave and longwave radiation within complex urban environment. The resultant  $T_{mrt}$  modelling shows that high radiant thermal load is confined to south-facing façades of buildings and open spaces. There are also considerable differences in radiant thermal load between various street orientations. Vegetation is found to be effective in reducing radiant thermal load since  $T_{mrt}$  is 8-19°C lower in areas shaded by vegetation. Findings of the present study suggest that mitigation measures such as using shading of buildings and

# PLEA 2015

BOLOGNA, ITALY  
09 -11 September 2015

vegetation should be adopted in areas with high radiant thermal load in order to maximize its shading effect. For locations with limited spaces, artificial shading devices such as arcades and extended canopies from buildings are recommended. Shading strategies should also consider local ventilation since it is very important to pedestrians' thermal comfort in Hong Kong.

**Keywords:** Heatwaves; heat stress; mean radiant temperature; SOLWEIG

## 1. Introduction

Global mean surface temperature is projected to increase by 2.6 to 4.8°C by the end of the 21st century under the high-emission scenario (IPCC, 2014). It is likely to increase the frequency, duration and magnitude of heatwave events in the future. In urban areas, due to the altered urban climatic conditions, the effect of heatwaves is often accentuated and caused substantial impacts on the health and well-being of urban population, especially elderly, infants and people with long-term cardiovascular and respiratory diseases (D'Ippoliti et al., 2010; Dousset et al., 2011). In high-density environment, the design of urban geometry has a great potential in mitigating outdoor heat stress since shading provided by surrounding structures are able to reduce radiant heat load (Emmanuel & Johansson, 2006; Krüger, Minella and Rasia, 2011). Appropriate design is capable of providing a more thermally comfortable environment under heatwave events.

Mean radiant temperature ( $T_{mrt}$ ) is one of the important parameters in assessing outdoor thermal comfort, which a function of all short- and long-wave radiation fluxes exposed by a human body (Mayer and Höpfe, 1987; Lindberg, Holmer, & Thorsson, 2008). It is defined as the 'uniform temperature of an imaginary enclosure in which radiant heat transfer from the human body equals the radiant heat transfer in the actual nonuniform enclosure' (ASHRAE 2001). Numerical modelling of  $T_{mrt}$  has been proved to accurately simulate the spatial variation of  $T_{mrt}$  within complex urban environment (Matzarakis, Rutz, & Mayer, 2007; Lindberg, Holmer & Thorsson, 2008; Lindberg & Grimmond 2011). Therefore, areas where heat stress occurs can be easily identified and the

effect of urban geometry on  $T_{mrt}$  can be examined.

In the present study, the spatial distribution of outdoor heat stress, using  $T_{mrt}$  as an indicator, is simulated using the SOLar and LongWave Environmental Irradiance Geometry (SOLWEIG) model during heatwave events. It aims to investigate the effect of urban geometry on the spatial distribution of  $T_{mrt}$  in high-density subtropical cities, using Hong Kong as a case study. The implications on the design of urban geometry, with regard to better outdoor thermal comfort, are also discussed.

## 2. Data and Methodology

### 2.1 Study Area

Hong Kong is located at the southeastern coast of China with latitude of 22.3°N. It has a subtropical climate, tending towards temperate during winter months (Hong Kong Observatory, 2012). Annual mean air temperature is 23.2°C with summer average of about 28°C. There is over 50% of possible sunshine from July to December with global solar radiation peaked at near 200Wm<sup>-2</sup> in July. As defined by the Hong Kong Observatory, days with daily maximum temperature over 33°C are classified as "very hot days". In the present study, the year of 2009 is chosen to investigate the spatial distribution of  $T_{mrt}$  under heatwave conditions it has the highest number of "very hot days" in the last 30 years (Fig 2). In particular, there are ten consecutive very hot days from 30th August to 8th September.

Two study areas are selected in the present study. The first is located in the central part of Hong Kong (Tsim Sha Tsui) characterized by dense and high-rise urban settings with long, narrow and parallel E-W streets. Despite of the vegetated slope in the northern part of the study area, there is no vegetation within the

street canyon. The second is an open square with trees planted along its edges. It is located in a residential neighbourhood (Lam Tin) in the urban fringe of Hong Kong.

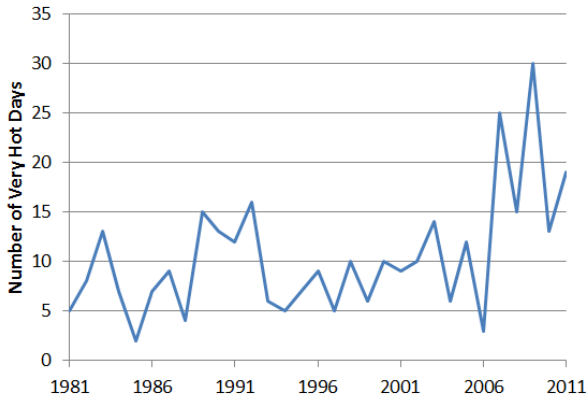


Fig 2: Number of very hot days (daily maximum temperature above 33°C) from 1981 to 2011.

## 2.2 SOLWEIG Model and Input Data

SOLWEIG (version 2014a) is a numerical model which simulates spatial variations of 3D radiation fluxes and  $T_{mrt}$  in complex urban

settings (Lindberg, Holmer, & Thorsson, 2008).  $T_{mrt}$  is derived from the modelling of six-directional (upward, downward and from the four cardinal points) short- and long-wave radiation fluxes. Shadow patterns and sky view factor (SVF) can also be generated by the model. The model is proven to provide accurate estimation of the radiation fluxes in different urban settings and weather conditions as well as in (Lindberg & Grimmond, 2011).

Terrain and meteorological data are two major inputs for the SOLWEIG model. Terrain data is in the form of a digital surface model (DSM) which includes both ground topography and building structures within the study area. The DSM, with a spatial resolution of 1 m, is derived from the digital elevation model of Hong Kong as well as building and podium data obtained from the Planning Department (Fig 3).

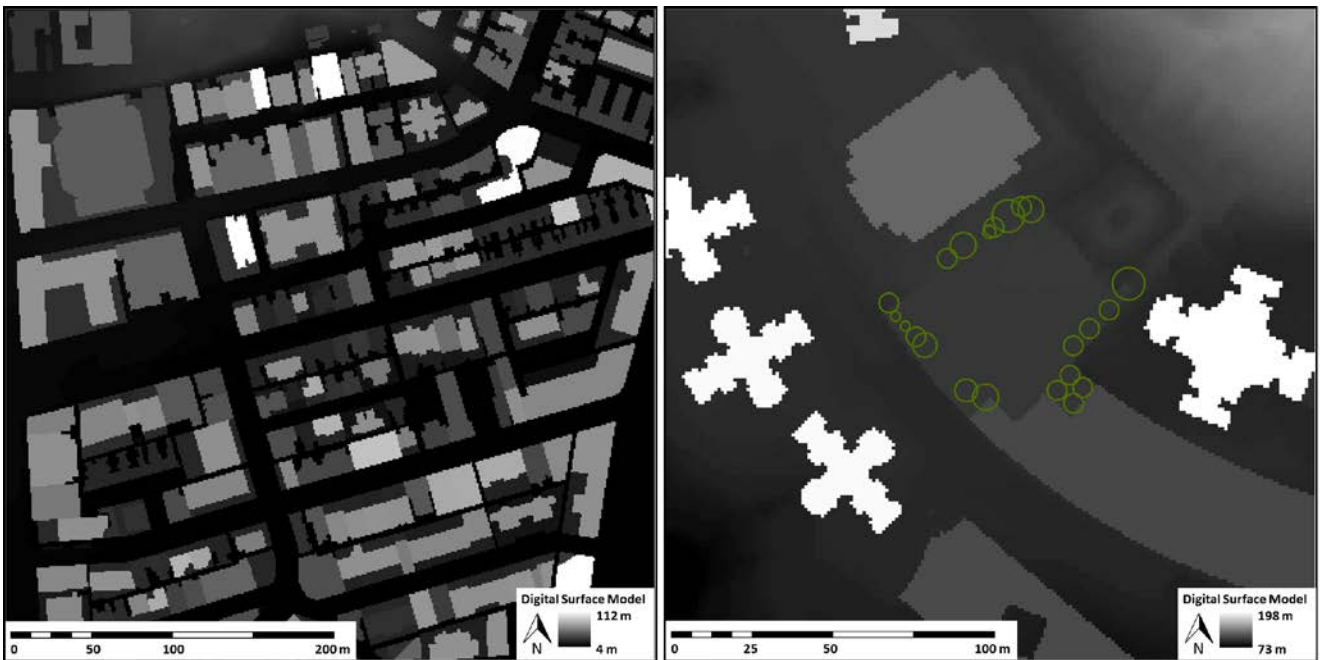


Fig 3: Digital surface model (DSM) of the two study areas. Green circles represent the size of tree crowns.

Meteorological inputs include air temperature ( $T_a$ ), relative humidity, global solar radiation recorded at two ground-level meteorological stations operated by the Hong Kong Observatory. Hourly data of the above meteorological variables were collected in 2008. The diffuse and direct components of solar radiation were calculated according to Lam and Li (1996). Field measurements were conducted within a street canyon on a clear autumn day (21 October 2014) for assessing the performance of the SOLWEIG model.

### 3. Results and Discussion

#### 3.1 Model Performance

Fig 4 shows the correlation between modelled and measured upward and downward shortwave and longwave radiation from the measurements sites. There is a good overall correspondence between the modelled and measured radiation fluxes with  $R^2$  values over 0.9. The root mean square errors (RMSE) for the four fluxes ( $K_{\downarrow}$ ,  $K_{\uparrow}$ ,  $L_{\downarrow}$  and  $L_{\uparrow}$ ) are 43.4, 18.3, 10.3 and 28.2  $\text{Wm}^{-2}$  respectively. The underestimation of downward and southward shortwave radiation (not shown) is believed to be associated with the different sky conditions of the measurement sites and meteorological stations. Nonetheless, it captures the diurnal variation of both shortwave and longwave radiation fluxes considerably well.

Fig 5 shows the scatterplot between modelled and measured values of  $T_{mrt}$  (15-min interval) using the data acquired from the measurement sites ( $n=52$ ), with an  $R^2$  value of 0.93. Modelled values are overestimated by about  $10^{\circ}\text{C}$  at noon due to the different sky conditions between the measurement site and the meteorological station at around noon.

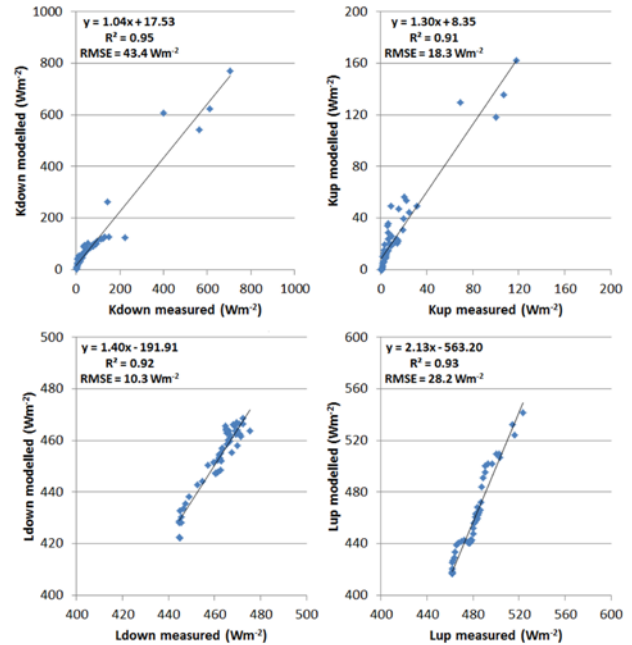


Fig 4: Correlation between modelled and measured downward ( $K_{\downarrow}$ , top left) and upward ( $K_{\uparrow}$ , top right) shortwave radiation fluxes, as well as downward ( $L_{\downarrow}$ , bottom left) and upward ( $L_{\uparrow}$ , bottom right) longwave radiation fluxes at the measurement sites.

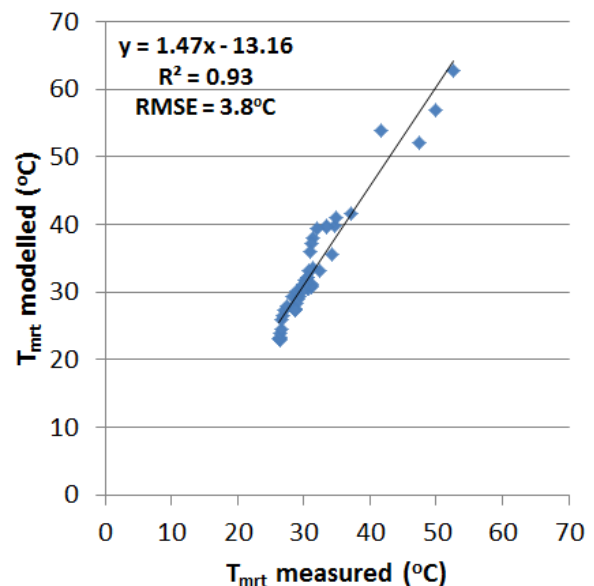


Fig 5: Correlation between modelled and measured  $T_{mrt}$ .



In the early afternoon, an overestimation of 5-7°C is observed due to the overestimated downward and southward longwave radiation. It is possibly explained by the lack of consideration of the thermal properties of building materials.

### 3.2 Spatial Variation of $T_{mrt}$ under Heatwave Conditions

In order to assess the spatial variation of  $T_{mrt}$  under heatwave conditions, the hourly  $T_{mrt}$  maps when daily maximum  $T_a$  is above 33°C were selected and averaged. The hourly average  $T_{mrt}$  map for Tsim Sha Tsui area is shown in Fig 1.  $T_{mrt}$  is generally higher in the open area located in the western part of the study area. Intense direct solar radiation reaching the ground surface is the primarily reason for such high  $T_{mrt}$  (Fig 6, left). Due to the high solar angle in the early afternoon in summer, the E-W streets are almost sunlit

except for the immediate front of the north-facing façades, resulting in hourly average  $T_{mrt}$  over 55°C. The higher level of direct solar radiation absorbed by building and ground surfaces leads to a substantial increase in  $T_{mrt}$ , as a result of increased long-wave radiation exposed to a standing body (Masmoudi and Mazouz 2004). It is shown by the higher downward longwave radiation emitted from sunlit surfaces (Fig 6, right). Lower  $T_{mrt}$  (about 40°C) is generally confined to north-facing building walls and the western side of the N-S streets since they are shaded by surrounding buildings. In addition, certain parts of the E-W streets exhibit lower  $T_{mrt}$  due to the presence of tall buildings. It suggests that there is a potential for using high-rise buildings to mitigate the high radiant load through shading under such heatwave conditions.

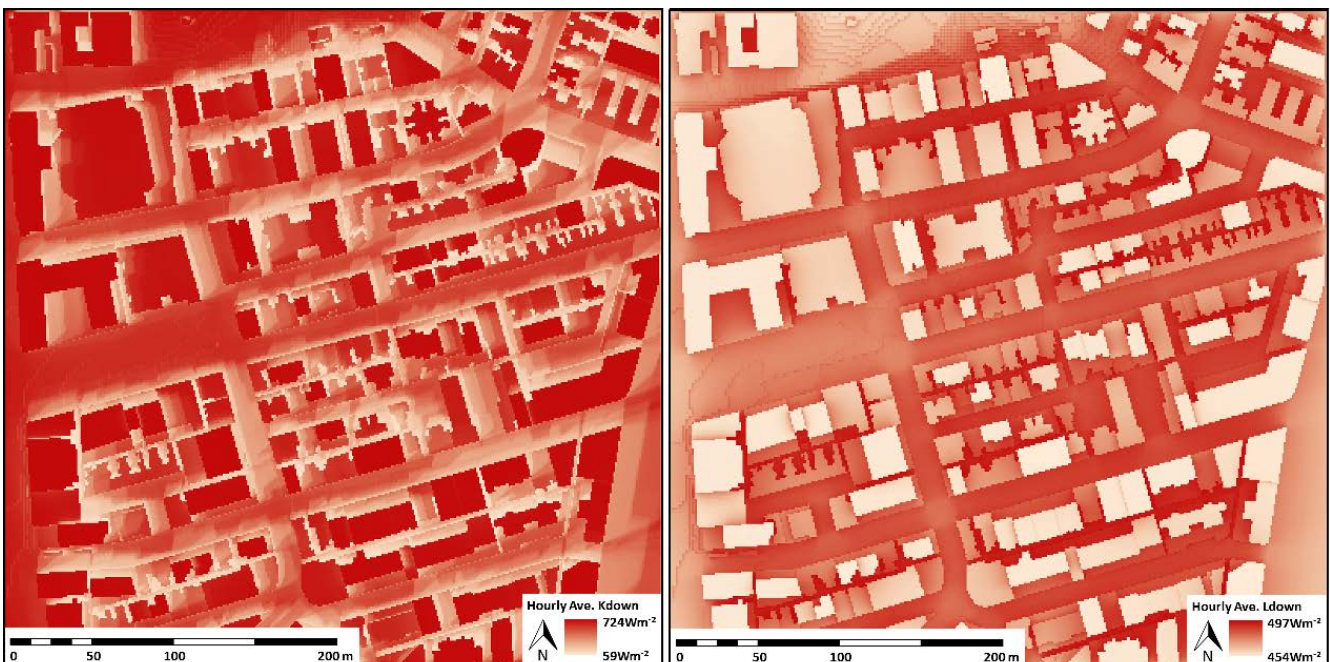


Fig 6: Spatial variation of downward shortwave (left) and longwave (right) radiation flux in Tsim Sha Tsui.

### 3.3 Effect of vegetation on $T_{mrt}$

Fig 1 shows the spatial variation of the hourly average  $T_{mrt}$  in the residential neighbourhood in Lam Tin. High-rise buildings on the western side provide extensive shading under heatwave conditions that the southwestern part of the open square is somewhat under shade. Hourly average  $T_{mrt}$  under tree shade in this part is about 8-9°C lower than the immediate surroundings. The difference in  $T_{mrt}$  due to the presence of trees is larger in sun-exposed areas (northeastern and central part of the open square). Hourly average  $T_{mrt}$  is at most 19°C higher than that under tree shade.

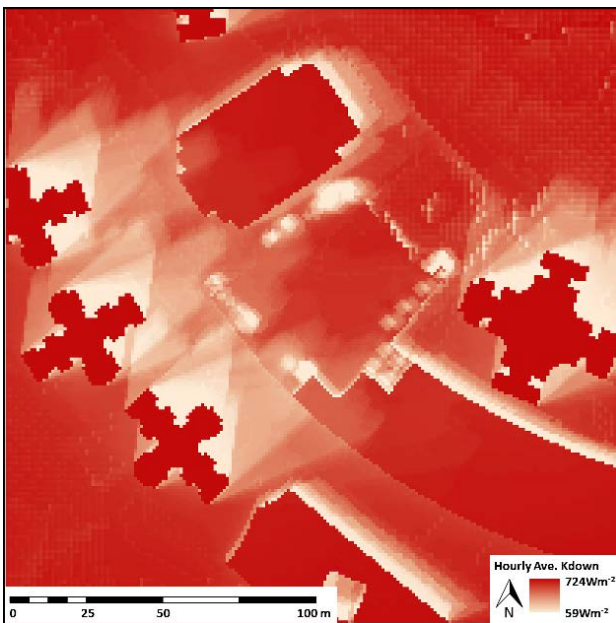


Fig 7: Spatial variation of downward shortwave in Lam Tin

In addition, scattered or sparsely planted trees are less effective in reducing  $T_{mrt}$  than a cluster of trees with more extensive coverage of tree crowns. Downward shortwave radiation is up to 500  $Wm^{-2}$  lower in the cluster of trees in the northern corner of the open square. In contrast, the scattered trees in the rest of the open square reduce downward shortwave radiation by only 250-300  $Wm^{-2}$ . It confirms the

high effectiveness of reducing radiant load in sun-exposed locations, especially using trees with dense tree crowns.

### 4. Conclusion

The SOLWEIG model was employed to examine the spatial variation of  $T_{mrt}$  in high-density subtropical urban environment under heatwave conditions. Field measurements confirm the capability of the model to simulate shortwave and longwave radiation fluxes and hence  $T_{mrt}$ . According to the simulation results, direct shortwave radiation is the predominant factor to the higher  $T_{mrt}$  in open areas than that of street canyons. High  $T_{mrt}$  is also observed in E-W street canyons, especially on the south-facing walls as a result of reflected short-wave radiation and long-wave radiation emitted from the building walls. N-S canyons are therefore more preferred in order to mitigate high  $T_{mrt}$ . Areas along sunlit building walls are also found to be hot spots where the highest  $T_{mrt}$  is observed. Shading is found to be an effective measure to mitigate high  $T_{mrt}$  as the lowest  $T_{mrt}$  is generally observed in the shaded areas along east-facing walls in the dense urban areas and under tree canopy in the residential neighbourhood. Findings of the present study suggest that shading of buildings and vegetation can improve radiant heat load at street level. However, the shading strategy has to be cautious about air ventilation in such a dense urban environment. Instead of increasing building height and density, using artificial shading devices such as overhanging façades and extended canopies from buildings is more preferred. Mitigation measures also include vegetation which lowers  $T_{mrt}$  through shading and evapotranspiration. Further work of the present study includes field measurements for better validation of the

models and the examination of the effect of different sky conditions on the spatial variation of  $T_{mrt}$  in the urban environment.

## 5. Acknowledgments

This study is supported by the Direct Grant of The Chinese University of Hong Kong. Dr Fredrick Lindberg from Department of Earth Science, University of Gothenburg is also acknowledged for his invaluable advice about the numerical modelling techniques employed in this study.

## 6. References

- ASHRAE. (2001). *ASHRAE fundamentals handbook 2001* (SI Edition). American Society of Heating, Refrigerating, and Air-Conditioning Engineers, USA.
- D'Ippoliti, D., Michelozzi, P., Marino, C., de'Donato, F., Menne, B., Katsouyanni, K., ... Perucci, C.A. (2010). The impact of heat waves on mortality in 9 European cities: results from the EuroHEAT project. *Environmental Health*, 9(1), 37.
- Dousset, B., Gourmelon, F., Laaidi, K., Zeghnoun, A., Giraudet, E., Bretin, P., ... Vandentorren, S. (2011). Satellite monitoring of summer heat waves in the Paris metropolitan area. *International Journal of Climatology*, 31, 313–323.
- Emmanuel, R., & Johansson, E. (2006). Influence of urban morphology and sea breeze on hot humid microclimate: the case of Colombo, Sri Lanka. *Climate Research*, 30, 189–200.
- Hong Kong Observatory, 2012. *Climate of Hong Kong*. Retrieved February 29, 2014, from [http://www.hko.gov.hk/cis/climahk\\_e.htm](http://www.hko.gov.hk/cis/climahk_e.htm)
- IPCC, 2014: *Climate Change 2014: Synthesis Report*. Contribution of Working Groups I, II and III to the Fifth Assessment Report of the Intergovernmental Panel on Climate Change [Core Writing Team, R.K. Pachauri and L.A. Meyer (eds.)]. IPCC, Geneva, Switzerland, 151 pp.
- Krüger, E., Minella, F.O., Rasia, F. (2011). Impact of urban geometry on outdoor thermal comfort and air quality from field measurements in Curitiba, Brazil. *Building and Environment*, 46 (3), 621–634.
- Lam, J.C., & Li, D.H.W. (1996). Correlation between global solar radiation and its direct and diffuse components. *Building and Environment*, 31(6), 527–535.
- Lindberg, F., & Grimmond, C.S.B. (2011). The influence of vegetation and building morphology on shadow patterns and mean radiant temperatures in urban areas: model development and evaluation. *Theoretical and Applied Climatology*, 105, 311–323.
- Lindberg, F., Holmer, B., Thorsson, S. (2008). SOLWEIG 1.0 - Modelling spatial variations of 3D radiant fluxes and mean radiant temperature in complex urban settings. *International Journal of Biometeorology*, 52, 697–713.
- Masmoudi, S., & Mazouz, S. (2004). Relation of geometry, vegetation and thermal comfort around buildings in urban settings, the case of hot arid regions. *Energy and Buildings*, 36, 710–719.
- Matzarakis, A., Rutz, F., & Mayer, H. (2007). Modelling radiation fluxes in simple and complex environments – application of the RayMan model. *International Journal of Biometeorology*, 51, 323–334.
- Mayer, H., & Höppe, P. (1987). Thermal comfort of man in different urban environments. *Theoretical and Applied Climatology*, 38, 43–49.